AuAg Nanosheets Assembled from Ultrathin AuAg Nanowires

Xun Hong, Chaoliang Tan, Juqing Liu, Jian Yang, Xue-Jun Wu, Zhanxi Fan, Zhimin Luo, Junze Chen, Xiao Zhang, Bo Chen, and Hua Zhang*

School of Materials Science and Engineering, Nanyang Technological University, 50 Nanyang Avenue, Singapore 639798, Singapore

S *Supporting Information*

ABSTRACT: Assembly of noble metal nanocrystals into free-standing two-dimensional (2D) nanostructures with a regular shape is still a challenge. Here we report the preparation of a novel 2D AuAg nanosheet with length of 1.50 ± 0.30 μm, width of 510 ± 160 nm, and thickness of ~100 nm via the assembly of ultrathin AuAg nanowires in the presence of the triblock copolymer Pluronic P123. The self-assembly of P123 and the fusion behavior of the nanowires during the assembly process are the key reasons for the formation of AuAg nanosheets in P123. Furthermore, the obtained AuAg nanosheet@P123 is used as the active material in a memory device that exhibits the write-once-read-many-times memory behavior.

Along with layered graphene and transition metal dichalcogenides with intrinsically layered crystal structures,[1-5] two-dimensional (2D) noble metal nanostructures have attracted increasing attention because of their unique properties and wide range of potential applications.[6-11] Recently, some novel 2D noble metal nanostructures have been synthesized via wet chemical synthesis methods. For example, for the first time, our group has synthesized Au square sheets with the hexagonal close-packed (hcp) rather than the normal face-centered cubic (fcc) structure by using graphene oxide as a template.[6] Meanwhile, ultrathin Pd[7] and Rh[8] nanosheets have also been synthesized, with carbon monoxide and formaldehyde as capping agents, respectively. Importantly, the aforementioned Pd and Rh nanosheets exhibit superior electrocatalytic and catalytic performances over the Pd and Rh spherical nanoparticles, respectively.

In addition to wet chemical synthesis methods, the assembly of nanocrystals to create novel nanostructures or complex architectures could be an alternative for preparation of 2D noble metal nanostructures.[12] Usually, the assembly of noble metal nanocrystals into 2D structures is achieved at liquid–liquid, liquid–air, or liquid–solid interfaces by the Langmuir–Blodgett technique or solvent-evaporation-induced self-assembly.[11-16] To date, noble metal nanoparticles or clusters with different sizes and shapes have been used as the building blocks for the synthesis of 2D noble metal nanostructures via self-assembly.[11-16] Unfortunately, the 2D noble metal nanostructures assembled from nanoparticles or clusters were mainly limited to the form of monolayer or multilayer films composed of noble metal nanocrystals. Recently, the controlled assembly of nanowires, which is important for the fabrication of functional electronic devices, has become one of the most active research areas.[17,18] Although great efforts have been devoted to the assembly of nanowires into highly aligned patterns, until now there has been no effective method to assemble nanowires into free-standing 2D nanosheets with a regular shape. Herein, for the first time, we report a novel type of AuAg nanosheets prepared from AuAg nanowires based on the combination of self-assembly of Pluronic P123 (EO20-PO70EO20) and fusion of AuAg nanowires. As a proof-of-concept, the AuAg nanosheet in P123, referred to as AuAg nanosheet@P123, is used as the active material in memory device, which exhibits the write-once-read-many-times (WORM) memory behavior.

In our experiments, the assembled AuAg nanosheets were prepared from ultrathin AuAg nanowires via a simple polymer-assisted assembly process in solution (Scheme 1). AuAg

Scheme 1. Synthesis of AuAg Nanosheets from Ultrathin AuAg Nanowires
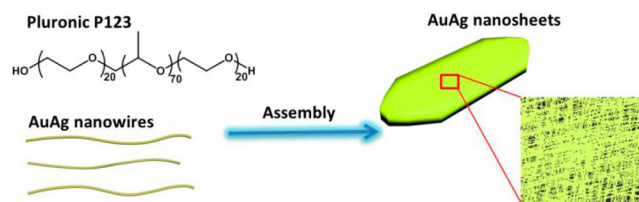
nanowires with diameter of 2–3 nm and length up to 1 μm, with a small amount of nanoparticles as the byproduct (Figure 1a), were prepared based on a previous report.[19] After the obtained AuAg nanowires were washed with water, they were redispersed in P123 aqueous solution (8 mg/mL). The AuAg nanowires mixed with P123 were then collected by centrifugation and redispersed in *N,N*-dimethylformamide (DMF) to induce the self-assembly of P123 and nanowires. Finally, the assembled composite was collected via centrifugation and washed with tetrahydrofuran (THF), and the assembled AuAg nanosheet@P123 with a regular shape was obtained.

Figure 1b shows a transmission electron microscopy (TEM) image of the assembled product, which is a sheet-like structure with length of 1.50 ± 0.30 μm and width of 510 ± 160 nm. Scanning electron microscopy (SEM) images and the corresponding size distribution histograms of the nanosheets are shown in the Supporting Information, Figure S1. The nanosheets can also be observed with an optical microscope (Figure S2). A high-angle annular dark-field scanning trans-
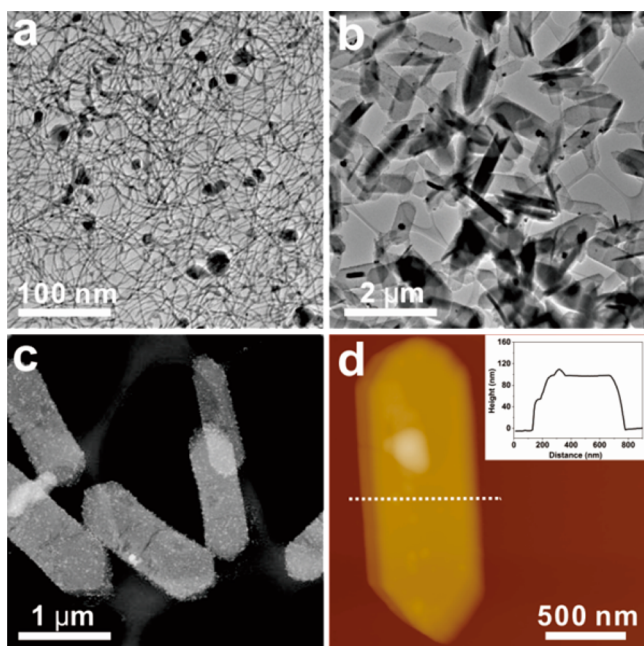
Figure 1. (a) TEM image of AuAg nanowires with small amount of nanoparticles as byproducts. (b) TEM image of the assembled AuAg nanosheets. (c) HAADF-STEM image of the assembled AuAg nanosheets. (d) AFM image of AuAg nanosheet. Inset: height profile of the dotted line.

mission electron microscopy (HAADF-STEM) image of the obtained nanosheets shows relatively homogeneous contrast, except for the bright dots arising from the nanoparticles, which are the byproduct generated in the synthesis of AuAg nanowires. This suggests that nanowires simultaneously self-assemble into the sheet structures. A typical atomic force microscopy (AFM) image indicates that the thickness of the assembled nanosheet is ca. 100 nm.

An enlarged TEM image of an AuAg nanosheet is shown in Figure 2a. It was found that the AuAg nanowires were broken into fragments and fused together to form connected networks. High-resolution TEM (HRTEM) analysis of the coalesced nanowires shows lattice fringes of 0.20 and 0.24 nm (Figure 2b), corresponding to the (200) and (111) planes of fcc AuAg, respectively. Furthermore, crystalline structures can be
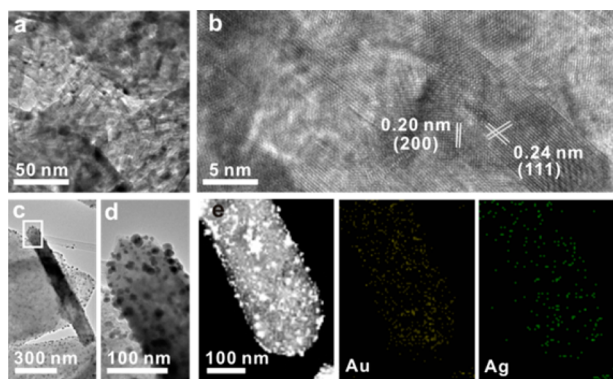

Figure 2. (a) Zoom-in TEM image of an AuAg nanosheet. (b) HRTEM image of a typical AuAg nanosheet. (c) Side-view TEM image of an AuAg nanosheet. (d) Zoom-in TEM image of the white rectangle in (c). (e) HAADF-STEM image of an AuAg nanosheet and the corresponding energy-dispersive X-ray spectroscopy mappings.

observed over the whole nanosheet (Figure S3). It is well known that the Au or AuAg nanowires with a diameter of ∼2 nm are easily broken.[20] Meanwhile, the fusion or cold-welding of Au nanoparticles has been demonstrated without thermal heating.[21−23] As a result, during the assembly process in our experiment, the AuAg nanowires could break into fragments and then fuse together. The shape of the structure remains after annealing at 350 °C in Ar atmosphere for 2 h (Figure S4). Figure S5 shows the UV−vis spectra of the AuAg nanowire and assembled AuAg nanosheet. A significant red shift in the absorption is observed after the assembly. A TEM side view of a nanosheet shows that the thickness of the nanosheet is ca. 100 nm (Figure 2c,d), which is consistent with the AFM measurement (Figure 1d). The elemental mapping of nanosheets was further used to confirm their composition, indicating the Au and Ag distribution in the nanosheets (Figure 2e).

The triblock copolymer P123, a commercially available surfactant, can self-assemble into different morphologies in selective solvents (Figures S6 and S7).[24,25] It usually forms dynamic core−shell micelles in water, composed of a hydrophobic PPO core and a hydrated PEO corona.[24] However, DMF is a good solvent for PPO but not for PEO.[25] Figure S8b shows the TEM images of the intermediate product collected after dispersion of the mixture of P123 and AuAg nanowires in DMF (see the Supporting Information for experimental details). The copolymer forms micelles and encapsulates AuAg nanowires after the addition of DMF, while the assembly process was not observed upon mixing P123 and AuAg nanowires in water (Figure S8a). P123 would aggregate in order to counteract the increasing interfacial tension when DMF was added.[25] Washing the aforementioned product with THF, which is a good solvent for both PPO and PEO of P123, led to the formation of regular sheet-like structures. The AuAg nanosheet@P123 (>80 wt% of AuAg, Figure S9) inherits the geometric features of the copolymer micelle. Although the anisotropic self-assembly of block copolymers has been observed by dissolving them in selective solvents,[26,27] the reason why such a regular sheet-like structure was formed is not clear yet.

Previous studies have demonstrated that the hybridization of noble metal nanoparticles with polymers to form composites could provide active materials for the fabrication of nonvolatile memory devices.[28−30] Therefore, our assembled 2D AuAg nanosheet@P123 could be a promising active material for data storage devices. As a proof-of-concept application, a memory device with a configuration of Au electrode/AuAg nanosheet@P123/indium−tin oxide (ITO)-covered glass was fabricated, using the hybrid nanosheets as the active layer (inset in Figure 3a). Based on the current−voltage (I−V) characteristics (Figure 3a), the device exhibits electrical bistable behavior. Starting with the low conductivity state (OFF state) in the device, the current state increased abruptly from 5.6×10^{-4} to 3.0×10^{-2} A at an applied positive voltage of +1.0 V (stage 1), indicating the electrical transition of the device from the OFF state to a high conductivity state (ON state), which can serves as the "writing" process for the device operation. The ON/OFF current ratio is over 1.3×10^2 at 0.5 V. After the transition, the device remained in the ON state during the subsequent positive sweep (stages 2 and 3), even if the power was switched off, indicating the nonvolatile nature of the memory effect. However, the OFF state could not be recovered by applying a reverse sweep voltage (stages 4 and 5), suggesting the
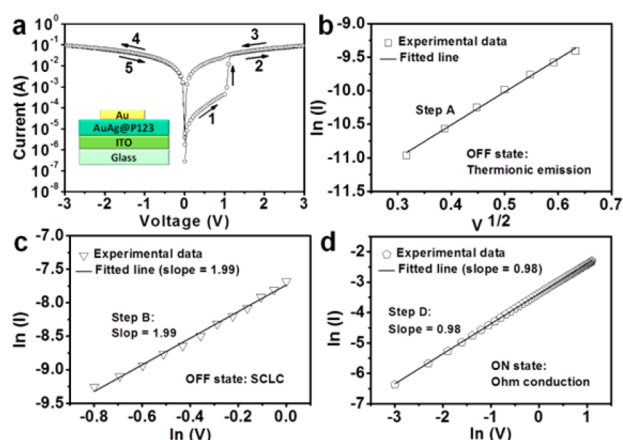
Figure 3. (a) I−V characteristics of the Au electrode/AuAg nanosheet@P123/ITO memory device. Inset: Schematic illustration of the fabricated memory device. Experimental data and fitted lines of the I−V characteristics: (b,c) OFF state and (d) ON state.

WORM memory behavior, which shows potential applications in permanent data storage.

To understand the carrier transport mechanism through the device, the I−V curves in both ON and OFF states were analyzed on the basis of the experimental data and theoretical models.[31] In the OFF state, a linear relation was observed in the plot of $\ln(I)$ vs $V^{1/2}$ at voltage from 0 to 0.4 V (Figure 3b). Such a linear characteristic indicates that the conduction mechanism probably arises from the thermionic emission,[29] and the OFF current is controlled by charge injection from the ITO electrode. After that, a linear relation was observed between $\ln(I)$ and $\ln(V)$ from 0.4 to 1.0 V, with a slope of 1.99 (Figure 3c), suggesting that space-charge-limited current dominates the carrier transport process.[32] This is understandable in terms of the electrical property of the active materials. Space charges occurred in the AuAg nanosheet@P123 due to the insulator property of P123 when charge carriers were sufficiently injected with increasing voltage. The I−V characteristic changed after the electrical switching to the ON state—a linear relation with a slope of 1.08 was observed between $\ln(I)$ and $\ln(V)$ (Figure 3d)—suggesting that the conduction mechanism may change to ohmic conduction in the ON state.

In summary, we report the preparation of a new type of AuAg nanosheets via the assembly of AuAg nanowires with the assistance of P123. By sequentially dissolving the P123 and AuAg nanowires in H_2O, DMF, and THF, the assembly behavior of P123 and fusion of AuAg nanowires can be observed, resulting in the formation of AuAg nanosheets in P123 with length of 1.50 ± 0.30 μm, width of 510 ± 160 nm, and thickness of ∼100 nm. Moreover, the obtained AuAg nanosheet@P123 can be used as the active material in a memory device, which exhibited the typical WORM switching behavior. It is expected that these novel assembled nanosheets may also have applications in catalysis reaction and energy storage.

■ ASSOCIATED CONTENT

ⓢ Supporting Information

Detailed experimental procedures; SEM, optical microscopy, TEM, and HRTEM images; and UV−vis spectrum of the AuAg nanosheets. This material is available free of charge via the Internet at http://pubs.acs.org.

■ AUTHOR INFORMATION

Corresponding Author
*hzhang@ntu.edu.sg

Notes
The authors declare no competing financial interest.

■ REFERENCES

(1) Novoselov, K. S.; Geim, A. K.; Morozov, S. V.; Jiang, D.; Zhang, Y.; Dubonos, S. V.; Grigorieva, I. V.; Firsov, A. A. Science 2004, 306, 666.
(2) Chhowalla, M.; Shin, H. S.; Eda, G.; Li, L. J.; Loh, K. P.; Zhang, H. Nat. Chem. 2013, 5, 263.
(3) Huang, X.; Zeng, Z. Y.; Zhang, H. Chem. Soc. Rev. 2013, 42, 1934.
(4) Zeng, Z. Y.; Yin, Z. Y.; Huang, X.; Li, H.; He, Q. Y.; Lu, G.; Boey, F.; Zhang, H. Angew. Chem., Int. Ed. 2011, 50, 11093.
(5) Tan, C. L.; Zhang, H. Chem. Soc. Rev. 2014, DOI: 10.1039/C4CS00182F.
(6) Huang, X.; Li, S. Z.; Huang, Y. Z.; Wu, S. X.; Zhou, X. Z.; Li, S. Z.; Gan, C. L.; Boey, F.; Mirkin, C. A.; Zhang, H. Nat. Commun. 2011, 2, 292.
(7) Huang, X. Q.; Tang, S. H.; Mu, X. L.; Dai, Y.; Chen, G. X.; Zhou, Z. Y.; Ruan, F. X.; Yang, Z. L.; Zheng, N. F. Nat. Nanotechnol. 2011, 6, 28.
(8) Duan, H. H.; Yan, N.; Yu, R.; Chang, C. R.; Zhou, G.; Hu, H. S.; Rong, H. P.; Niu, Z. Q.; Mao, J. J.; Asakura, H.; Tanaka, T.; Dyson, P. J.; Li, J.; Li, Y. D. Nat. Commun. 2014, 5, 3093.
(9) Qin, H. L.; Wang, D.; Huang, Z. L.; Wu, D. M.; Zeng, Z. C.; Ren, B.; Xu, K.; Jin, J. J. Am. Chem. Soc. 2013, 135, 12544.
(10) Andoy, N. M.; Zhou, X. C.; Choudhary, E.; Shen, H.; Liu, G. K.; Chen, P. J. Am. Chem. Soc. 2013, 135, 1845.
(11) Wu, Z. N.; Dong, C. W.; Li, Y. C.; Hao, H. X.; Zhang, H.; Lu, Z. Y.; Yang, B. Angew. Chem., Int. Ed. 2013, 52, 9952.
(12) Gong, J. X.; Li, G. D.; Tang, Z. Y. Nano Today 2012, 7, 564.
(13) Nie, Z. H.; Petukhova, A.; Kumacheva, E. Nat. Nanotechnol. 2010, 5, 15.
(14) Sánchez-Iglesias, A.; Grzelczak, M.; Pérez-Juste, J.; Liz-Marzán, L. M. Angew. Chem., Int. Ed. 2010, 49, 9985.
(15) Tao, A. R.; Huang, J. X.; Yang, P. D. Acc. Chem. Res. 2008, 41, 1662.
(16) Shevchenko, E. V.; Talapin, D. V.; Kotov, N. A.; O'Brien, S.; Murray, C. B. Nature 2006, 439, 55.
(17) Liu, J. W.; Liang, H. W.; Yu, S. H. Chem. Rev. 2012, 112, 4770.
(18) Yao, J.; Yan, H.; Lieber, C. M. Nat. Nanotechnol. 2013, 8, 329.
(19) Wang, Y.; Wang, Q. X.; Sun, H.; Zhang, W. Q.; Chen, G.; Wang, Y. W.; Shen, X. S.; Han, Y.; Lu, X. M.; Chen, H. Y. J. Am. Chem. Soc. 2011, 133, 20060.
(20) Wang, C.; Sun, S. H. Chem.—Asian J. 2009, 4, 1028.
(21) Xu, J.; Wang, Y. W.; Qi, X. Y.; Liu, C. C.; He, J. T.; Zhang, H.; Chen, H. Y. Angew. Chem., Int. Ed. 2013, 52, 6019.
(22) Lu, Y.; Huang, J. Y.; Wang, C.; Sun, S. H.; Lou, J. Nat. Nanotechnol. 2010, 5, 218.
(23) Ding, M. N.; Sorescu, D. C.; Kotchey, G. P.; Star, A. J. Am. Chem. Soc. 2012, 134, 3472.
(24) Petrov, P.; Yuan, J. Y.; Yoncheva, K.; Müller, A. H. E.; Tsvetanov, C. B. J. Phys. Chem. B 2008, 112, 8879.
(25) Denkova, A. G.; Bomans, P. H. H.; Coppens, M. O.; Sommerdijk, N. A. J. M.; Mendes, E. Soft Matter 2011, 7, 6622.

(26) Cui, H. G.; Chen, Z. Y.; Zhong, S.; Wooley, K. L.; Pochan, D. J. *Science* **2007**, *317*, 647.

(27) Zhong, Z.; Lee, H.; Shen, S.; Gedanken, A. *Soft Matter* **2009**, *5*, 2558.

(28) Lee, J. S.; Cho, J.; Lee, C.; Kim, I.; Park, J.; Kim, Y. M.; Shin, H.; Lee, J.; Caruso, F. *Nat. Nanotechnol.* **2007**, *2*, 790.

(29) Prakash, A.; Ouyang, J. Y.; Lin, J. L.; Yang, Y. *J. Appl. Phys.* **2006**, *100*, 054309.

(30) Leong, W. L.; Lee, P. S.; Lohani, A.; Lam, Y. M.; Chen, T.; Zhang, S.; Dodabalapur, A.; Mhaisalkar, S. G. *Adv. Mater.* **2008**, *20*, 2325.

(31) Ling, Q. D.; Liaw, D. J.; Zhu, C. X.; Chan, D. S. H.; Kang, E. T.; Neoh, K. G. *Prog. Polym. Sci.* **2008**, *33*, 917.

(32) Lee, J.; Hong, W. G.; Lee, H. *Org. Electron.* **2011**, *12*, 988.